

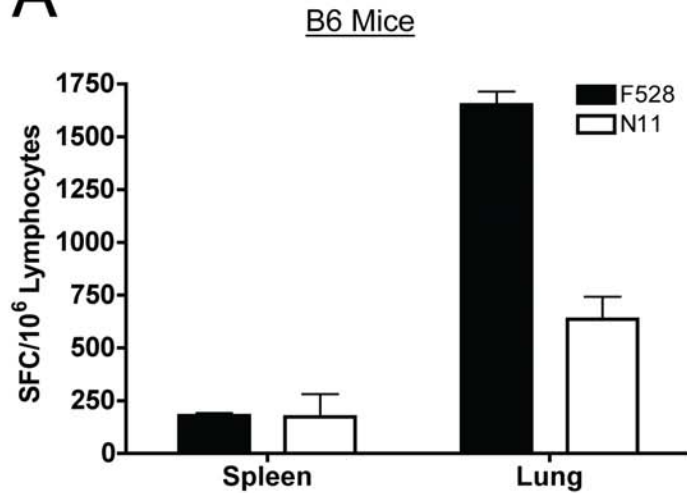
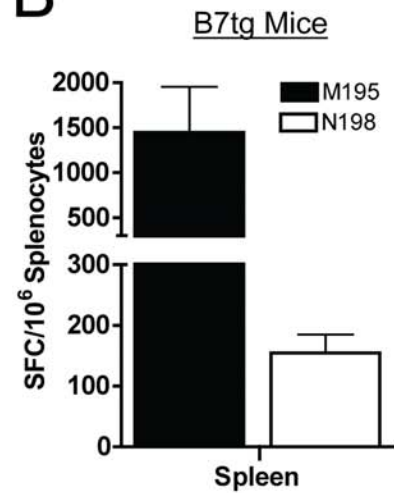
SUPPLEMENTARY FIGURES

Viral Acute Lower Respiratory Infections Rapidly Impair CD8⁺ T Lymphocyte Functions Through the PD-1/PD-L1 Pathway

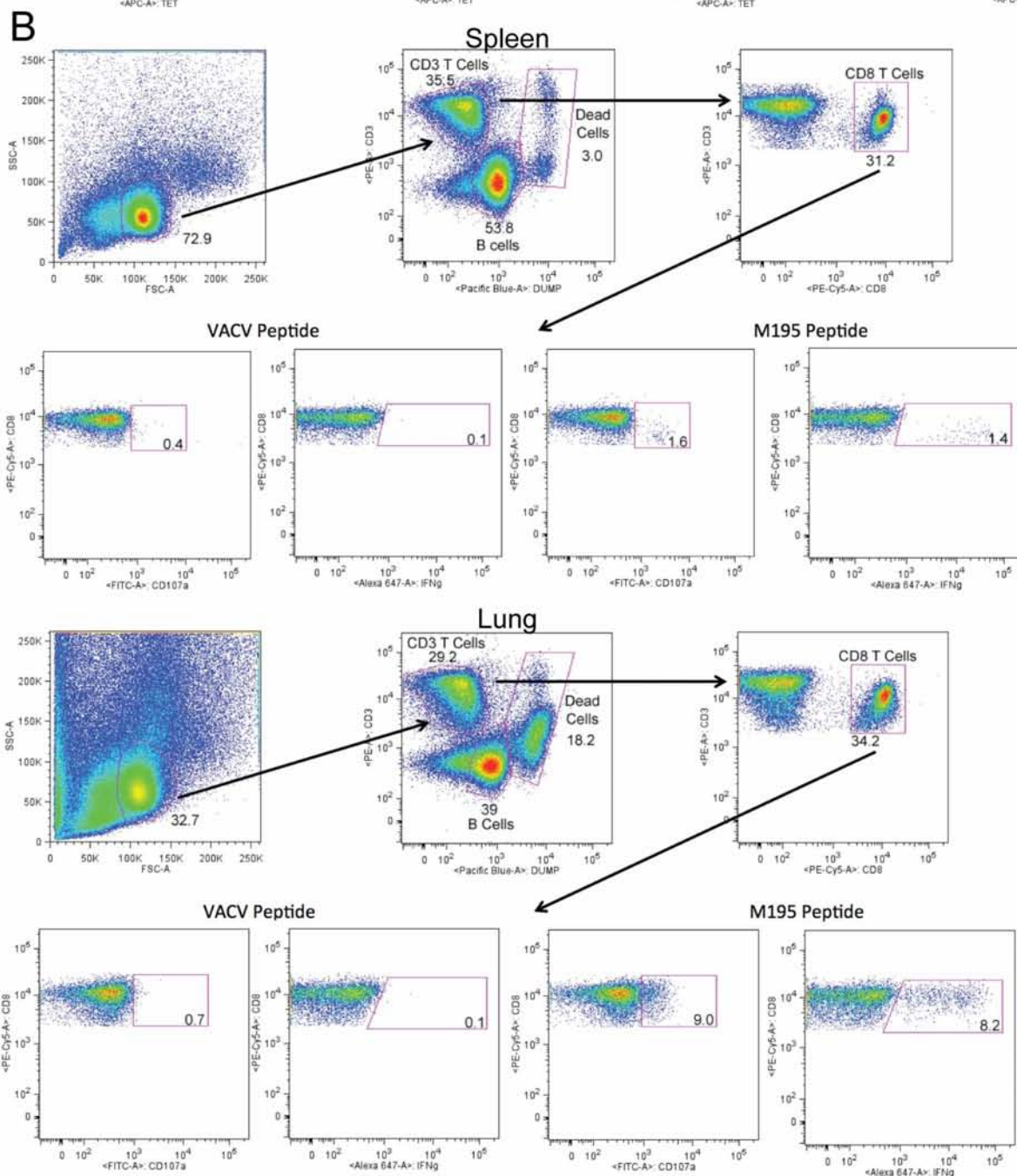
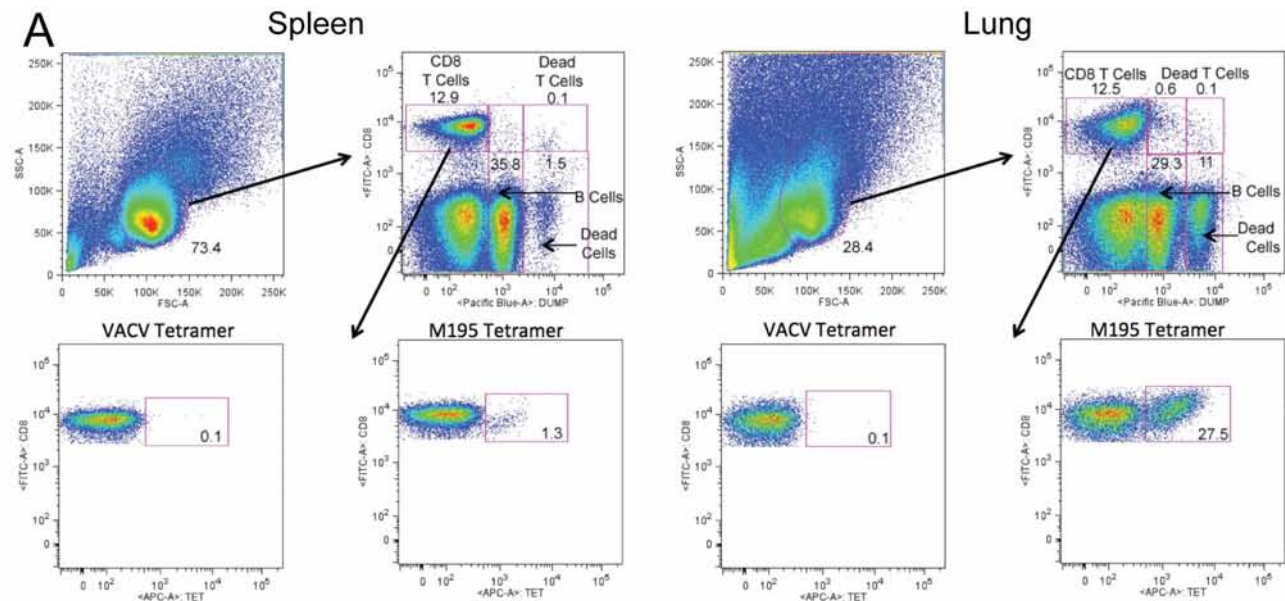
John J. Erickson¹, Pavlo Gilchuk¹, Andrew K. Hastings¹, Sharon J. Tollefson², Monika Johnson¹, Melissa B. Downing¹, Kelli L. Boyd¹, Joyce E. Johnson¹, Annette S. Kim¹, Sebastian Joyce¹ and John V. Williams.^{1,2,3}

Departments of ¹Pathology, Microbiology & Immunology and ²Pediatrics,

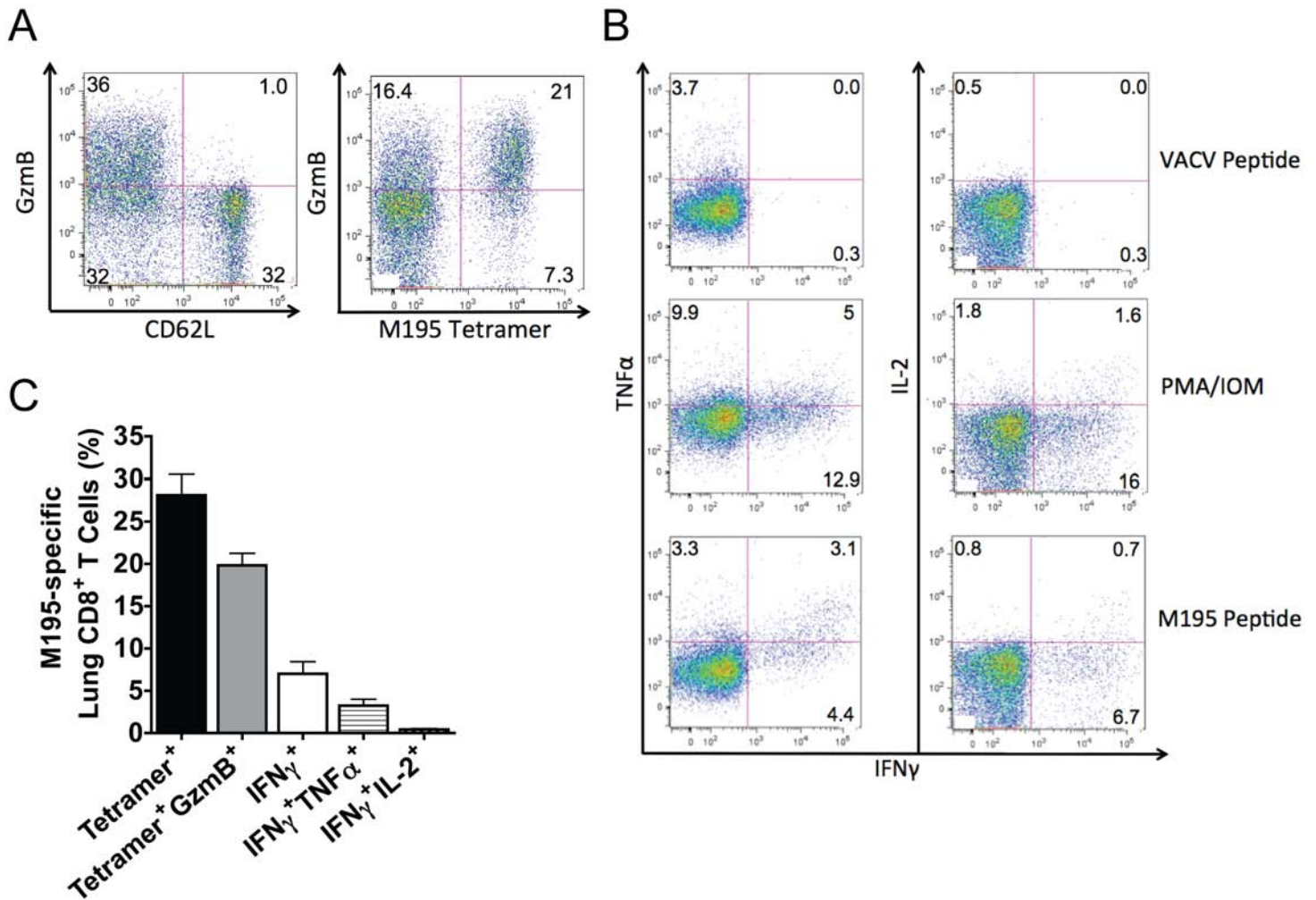
Vanderbilt University School of Medicine, Nashville, TN 37232

A**B**

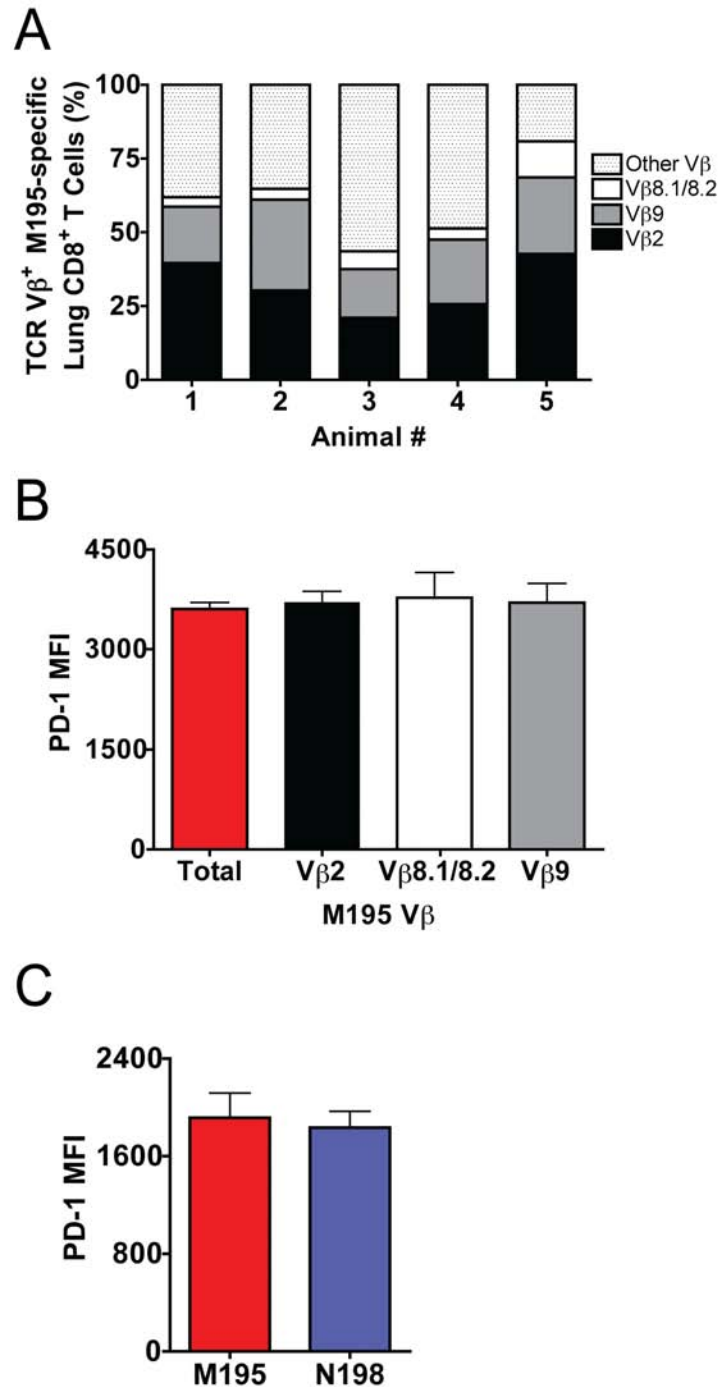
Supplementary Figure 1 Identification of HMPV T_{CD8} epitopes. C57BL/6 (B6) (**A**) or B6-Kb⁰Db⁰;B7.2 transgenic (B7tg) (**B**) mice were infected with HMPV and then spleen or lung lymphocytes were isolated 10 days post-infection. HMPV immune cells were screened for IFN γ release via ELISPOT assay using H2-D^b/H2-K^b (**A**) or HLA-B*0702 predictopes (**B**). Results indicate spot forming cells (SFC) per 10⁶ splenocytes or lung lymphocytes following stimulation with the indicated peptide (background subtracted). Results for only the top two epitopes are shown. Data in (**A**) are combined from at least 2 independent experiments with 3-5 individual mice per experiment while data in (**B**) are combined from 3 independent experiments with 5 pooled mouse spleens per experiment.



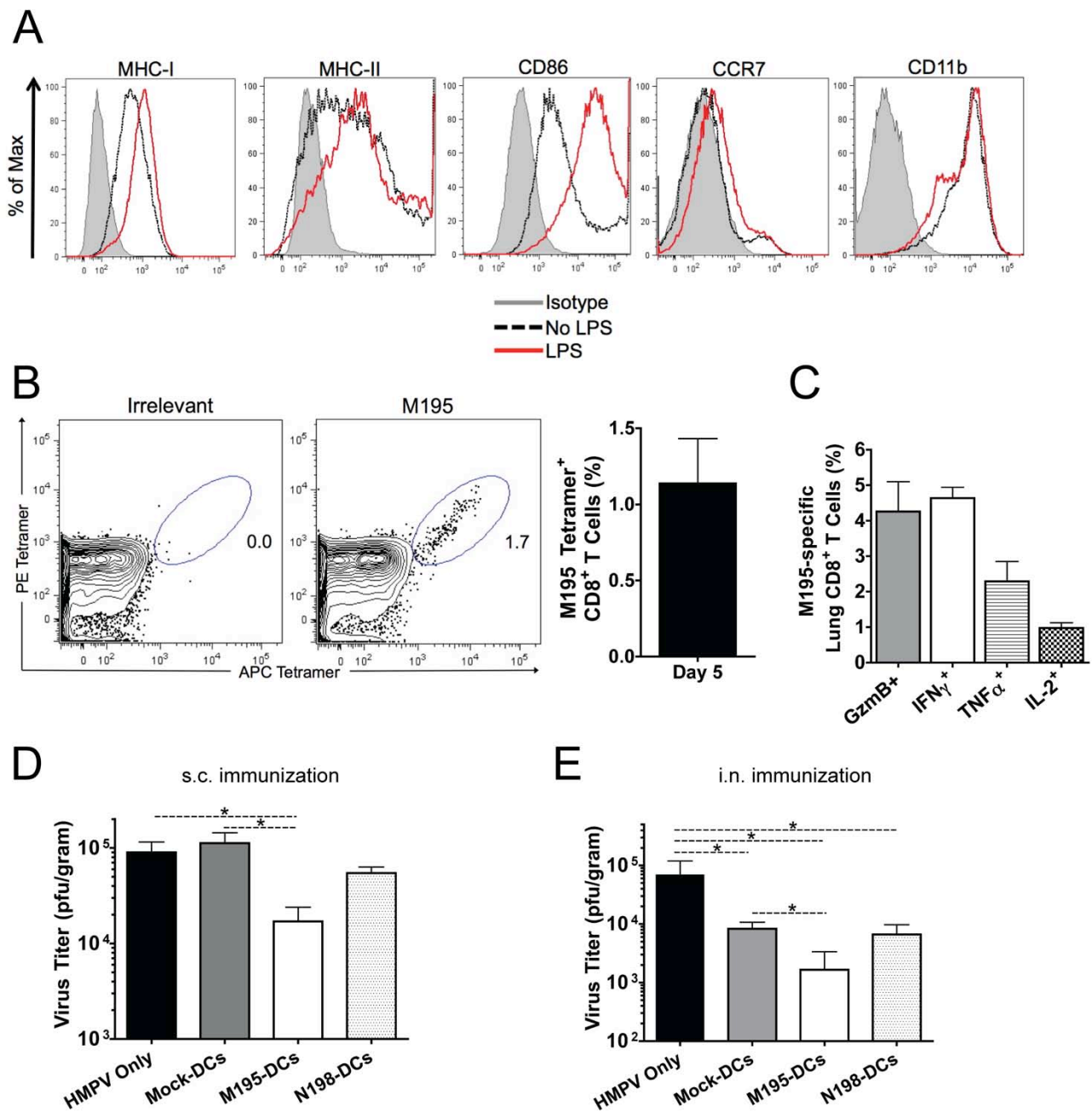
Supplementary Figure 2 Flow cytometry gating strategy for experiments in Figures 2-9. For both tetramer staining **(A)** and intracellular cytokine staining (ICS) **(B)**, lung or spleen cells were surface stained for CD8 and CD19. For ICS, cells were also stained for CD3. Dead cells were excluded using an amine reactive dye. For tetramer analysis, cells were stained directly *ex vivo*. For ICS, cells were first restimulated for 6 hours with 10 μ M peptide in the presence of anti-CD107a antibody and the protein transport inhibitors brefeldin A and monensin before surface and intracellular staining for IFN γ . For B7tg mice, background values obtained from staining with an irrelevant VACV-specific tetramer or restimulation with the same VACV peptide (A34R₈₂₋₉₀, the immunodominant epitope for VACV in B7tg mice) were subtracted. For B6 mice, background values obtained from staining with IAV NP366 tetramer or restimulation with the same peptide were subtracted. 10,000-20,000 CD8⁺ T cells were counted per lung or spleen.



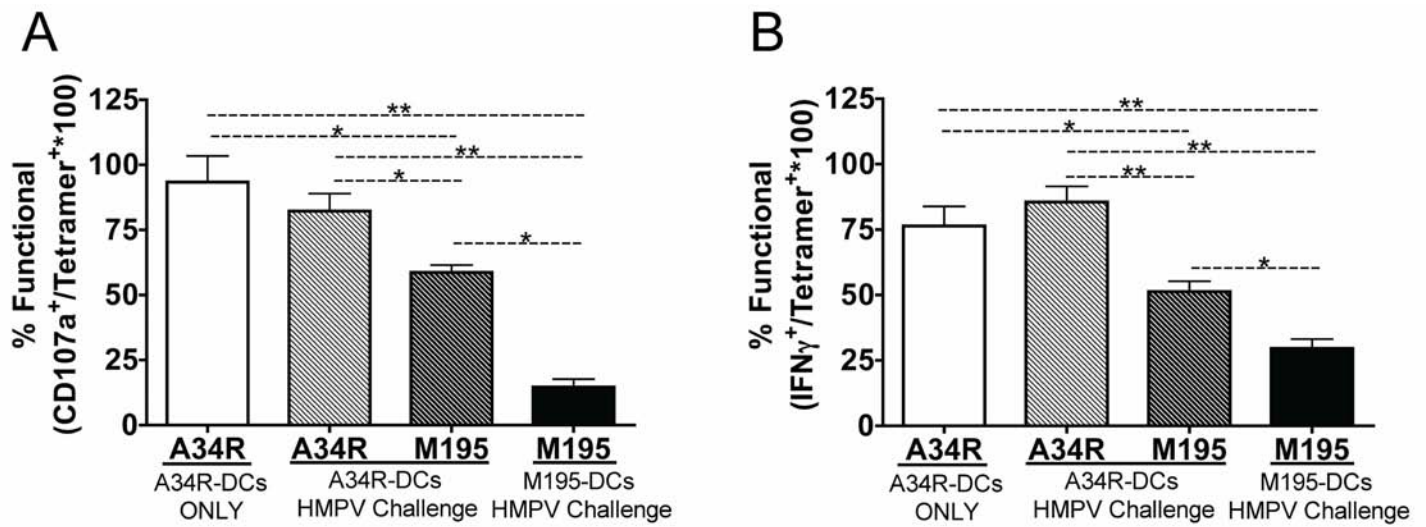
Supplementary Figure 3 HMPV-specific pulmonary T_{CD8}s are impaired for multiple key effector functions. B7tg mice were infected with HMPV and lung lymphocytes were isolated 10 days post-infection. **(A)** Lung lymphocytes were stained directly *ex vivo* with M195 tetramer and anti-CD62L followed by intracellular staining for granzyme B (GzmB). GzmB⁺ T_{CD8}s were identified by exclusionary gating from the CD62L⁺ population, which are GzmB⁻ naïve or central memory cells (left flow plot). The same GzmB electronic gate was applied to M195 tetramer⁺ cells in order to identify GzmB⁺ M195-specific T_{CD8}s (right flow plot). **(B)** Lung lymphocytes from the same mice were restimulated with an irrelevant VACV peptide, mitogen (PMA/ionomycin) or M195 peptide. Flow plots are gated on CD8⁺ T cells and display IFNγ versus TNFα (left column) or IFNγ versus IL-2 (right column). **(C)** Summary of all lung T_{CD8} functions examined in **(A)** and **(B)**. One representative experiment of two independent experiments with 5 individual mice per experiment is shown.



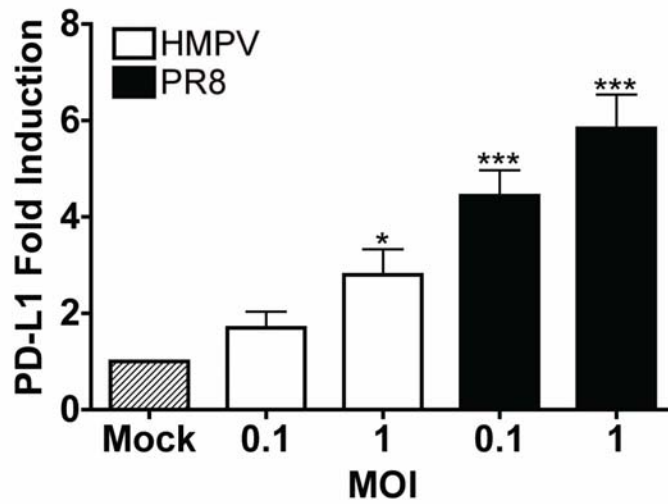
Supplementary Figure 4 HMPV-specific T_{CD8s} are polyclonal with indistinguishable PD-1 expression between different TCR Vβ families and different epitopes. B7tg mice were infected with HMPV and lung lymphocytes were isolated 10 days post-infection. **(A)** Lung cells were stained with M195 tetramer and a panel of Vβ-specific antibodies. The three most common TCR Vβ chains are shown for each individual mouse. **(B)** PD-1 mean fluorescence intensity (MFI) for total M195-specific T_{CD8s} (red bars) is displayed alongside the MFI for individual Vβ families. **(C)** PD-1 MFI is shown for either M195- (red bar) or N198- (blue bar) specific T_{CD8s}. One representative experiment of two independent experiments with 5 individual mice per experiment is shown.



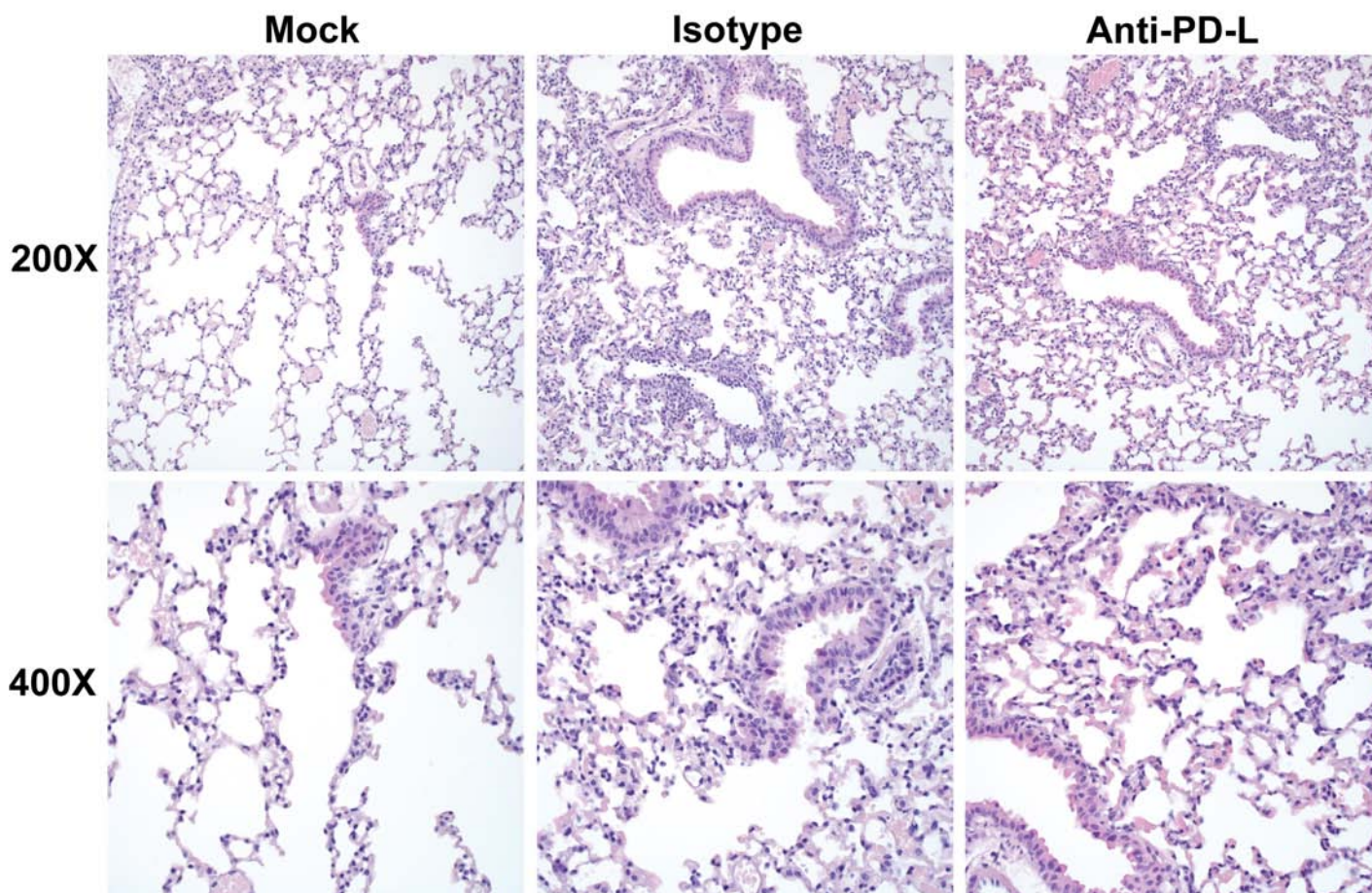
Supplementary Figure 5 Intranasal DC immunization elicits polyfunctional T_{CD8s} capable of protecting mice from challenge infection. **(A)** Bone marrow-derived DCs were either not matured (dotted black line) or matured with LPS (solid red line) and then stained for several maturation markers. **(B and C)** B7tg mice were immunized intranasally with M195-loaded, LPS-matured DCs. **(B)** At day 5 post-immunization, lung lymphocytes were isolated and stained with either dual color irrelevant (left flow plot) or M195 (right plot) tetramers to increase the sensitivity of detection. Bar graph displays combined data from several individual mice. **(C)** At day 7 post-immunization, lung lymphocytes were isolated and stained for intracellular GzmB or restimulated with M195 peptide and stained for intracellular IFN γ , TNF α and IL-2. **(D and E)** B7tg mice were immunized subcutaneously (s.c.) **(D)** or i.n. **(E)** with DCs loaded with M195 (M195-DCs), N198 (N198-DCs) or an irrelevant vaccinia virus peptide (Mock-DCs). Control animals were unimmunized (HMPV Only). At day 14 post-immunization, mice were challenged with HMPV and 5 days later lungs were harvested for viral titration. Data in **(A and B)** are representative of at least two independent experiments. Data in **(C-E)** are combined from 2 or 3 independent experiments with 4-5 individual mice per group per experiment. * $p < 0.05$ (one-way ANOVA with Bonferroni post-test)



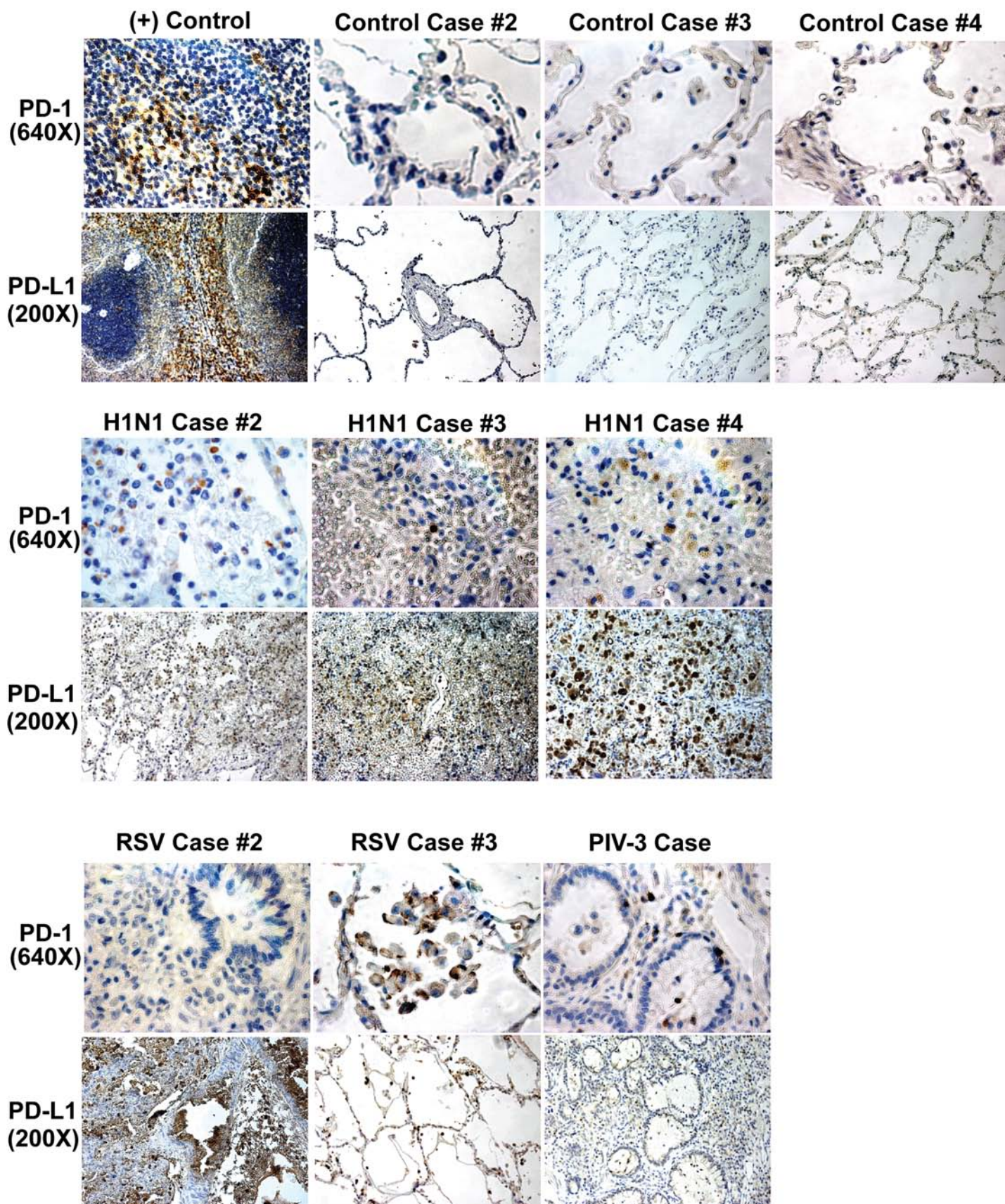
Supplementary Figure 6 Cognate viral antigen is required for pulmonary T_{CD8} functional impairment. From the same experiment in Figure 4A, the percentage of functional epitope-specific T_{CD8s} was calculated by dividing the percentage of CD8⁺ T cells that are either CD107a⁺ (**A**) or IFN γ ⁺ (**B**) by the percentage of CD8⁺ T cells that are tetramer⁺ for the same epitope. * $p < 0.05$, ** $p < 0.005$ (one-way ANOVA with Bonferroni post-test).



Supplementary Figure 7 Viral infection of human bronchial epithelial cells induces PD-L1 upregulation. Human bronchial epithelial cells (BEAS-2b line) were either mock infected or infected with the given multiplicities of infection (MOI) for HMPV or IAV (strain A/34/PR/8). 48 hours later cells were surface stained for PD-L1 and analyzed by flow cytometry. The fold induction of PD-L1 MFI over mock infection is shown. Data are combined from 4 independent experiments. Asterisks indicate statistically higher PD-L1 levels compared to mock infected cells. * $p < 0.05$, *** $p < 0.0005$ (two-tailed, Student's t-test).



Supplementary Figure 8 Anti-PD-L treatment does not exacerbate lower airway pathology. Mice were treated and infected as described in Figure 6. Lung sections from Isotype or Anti-PD-L treated mice were H&E stained. Images are representative of 4-5 individual mice per group. Original magnifications as indicated.



Supplementary Figure 9 PD-1 and PD-L1 are expressed in the lower airways of patients with severe 2009 H1N1 pandemic IAV, RSV or PIV-3 infection. Lung autopsy specimens were stained with anti-PD-1 or anti-PD-L1 antibodies. Tonsil or spleen tissues were used as positive controls for PD-1 or PD-L1, respectively. “Control Cases” are from patients with non-pulmonary disease (Case #2 – 33-year old male; Case #3 – 57-year old male; Case #4 – 37-year old male). “H1N1 Cases” are from patients infected with 2009 H1N1 pandemic IAV (Case #2 – 31-year old male; Case #3 – 41-year old male; Case #4 – 19-month old female). “RSV Cases” are from patients infected with seasonal RSV (Case #2 – 2-year old male; Case #3 – 63-year old male). “PIV-3 Case” is from a 7-year old male infected with PIV-3. Original magnifications as indicated.